Session 16 Overview

MEMS and Sensors

Chair: Farrokh Ayazi, Georgia Institute of Technology, Atlanta, GA

Associate Chair: Hirofumi Sumi, Sony, Kanagawa, Japan

This session presents recent advances in microsystems technology for applications in sensing and wireless communication. Advanced micromachined devices are interfaced with CMOS electronics to achieve state-of-the-art performance. Circuit techniques and material properties are exploited to potentially eliminate the need for expensive calibration in sensors. The nine presentations in this session illustrate precision sensing of acceleration, temperature, electrostatic field, magnetic field, and images at low-power and small form factor. In addition, high-performance CMOS interfaces for gas sensing and MEMS-based transmitters are presented. These technologies enable direct and seamless interfacing of digital computers to the real world.

The first paper of the session (16.1) presents significant advances in micro-g acceleration sensing with a large dynamic range. The low noise is achieved using an SOI substrate with thick silicon seismic mass, and high sensitivity is achieved by reducing gaps between sense electrodes through post-deposition of LPCVD polysilicon onto the electrodes, thus realizing an acceleration resolution of $4\mu g/\sqrt{Hz}$. In Paper 16.2, the first programmable MEMS FSK transmitter is realized using a frequency-tunable MEMS resonator in the feedback loop of a fractional-N frequency synthesizer. The variable frequency oscillator (2 to 437MHz) outperforms the quartz crystal based oscillator for mobile wireless platform application. The MEMS chip presented in Paper 16.3 demonstrates electrostatic field sensing. This technique is less-frequently discussed in the context of MEMS and can be applied to xerography, non-contact voltage sensing and precision electrometers. The charge induced on a micro-machined resonant polysilicon shutter, as it cuts through the electrostatic field, is amplified and synchronously demodulated to quantify the electrostatic field. A simple CMOS circuit architecture based on a relaxation oscillator is presented in Paper 16.4 for temperature control of a gas sensor. A ±2.5˚C accuracy over the 100 to 400˚C range is realized and integrated with the readout circuit to give 0.5% linearity and 114dB dynamic range.

Paper 16.5 presents a new technique of temperature sensing exploiting the temperature dependence of thermal diffusivity in bulk silicon. The sensor accuracy is comparable to the state-of-the-art (±0.5˚C), but it only requires low-cost batch calibration rather than expensive trimming of individual devices. An integrated magnetic sensor incorporating digital compensation for package-induced mechanical stress is presented in Paper 16.6.

A record 200dB dynamic range is achieved in the image sensor presented in Paper 16.7. The image sensor presented in 16.8 is back illuminated and achieves 34% better sensitivity than a conventional device. A laser radar imager using two layers of fully depleted SOI circuits integrated with a single photon detector is presented in Paper 16.9.

 1-4244-0079-1/06/$20.00

16.1 A 4.5mW Closed-Loop $\Delta\Sigma$ Micro-gravity CMOS-SOI Accelerometer **1:30 PM**

B. Vakili Amini, Georgia Institute of Technology, Atlanta, GA

A force-rebalanced high-order $\Delta\Sigma$ micro-g accelerometer has been implemented in CMOS-SOI. The measured acceleration resolution is $4\mu g/\sqrt{Hz}$, which is equivalent to a capacitive resolution of 2aF with a dynamic range of 95dB at 20Hz (resolution BW=3Hz). Measured sensitivity is 5pF/g (gain of 30V/g). The IC consumes 4.5mW from a 3V supply and uses $2.25mm^2$.

16.2 A Programmable MEMS FSK Transmitter **2:00 PM**

W-T. Hsu, Discera, Ann Arbor, MI

An FSK transmitter is modulated by changing the polarization voltage of a micromechanical resonator. The transmitter frequency can be programmed from 2 to 437MHz with 1ppm accuracy. The transmitter has 6X greater frequency deviation than quartz-based FSK modulators, 20kb/s data rate, and total 8ppm frequency variation from -40 to 85°C.

16.3 A Self-Resonant MEMS-based Electrostatic Field Sensor with $4V/m/\sqrt{Hz}$ Sensitivity **2:30 PM**

K. Lundberg, Massachusetts Institute of Technology, Cambridge, MA and Keeling Flight Hardware, Weston, MA

An electric-field sensor is presented for applications such as xerography. The sensor architecture combines a vibrating MEMS structure with synchronous detection-based electronics. Prototyped in a MEMS process, the noise floor is $4.0V/m/\sqrt{Hz}$ and the INL is 20V/m over a range of +/-700kV/m, an order-of-magnitude improvement over existing MEMS devices.

16.4 A CMOS Interface for a Gas-Sensor Array with a 0.5% Linearity over the $500k\Omega$-to-$1G\Omega$ Range and ±2.5°C Temperature Control Accuracy **2:45 PM**

M. Malfatti, Center for Scientific and Technological Research, Trento, Italy

The interface IC includes 8 read-out channels and 2 closed-loop temperature control circuits, is fabricated in 0.35µm 2P4M CMOS and dissipates 27mW from a 3.3V supply. The read-out structure, based on a controlled oscillator, achieves a 0.5% linearity and a SNR>48dB over the $500k\Omega$-to-$1G\Omega$ sensor resistance range with a 114dB DR. The temperature control systems maintain a 100°C gradient in the range 100 to 400°C with ±2.5°C accuracy.

16

16.5 A CMOS Temperature-to-Frequency Converter with ±0.5°C (3σ) Inaccuracy from –40 to 105°C **3:15 PM**

K. Makinwa, Delft University of Technology, Delft, The Netherlands

A temperature-to-frequency converter implemented in a standard CMOS process only requires a low-cost batch calibration. Its output frequency is determined by the process-independent (but temperature-dependent) thermal diffusivity of bulk silicon. The converter's inaccuracy is less than ±0.5°C (3σ) over the extended industrial temperature range from –40 to 105°C.

16.6 An Integrated Magnetic Sensor with Two Continuous-Time $\Delta\Sigma$ Converters and Stress Compensation Capability

M. Motz, Infineon, Villach, Austria **3:45 PM**

A linear 4kHz Hall sensor in 0.6µm BiCMOS has digital 3rd-order temperature compensation, a DR of 90dB and an offset of 50µT. It uses a chopped 3rd-order multibit CT-$\Delta\Sigma$ ADC including an up/down counter loop and bandgap-based compensation for stability and accuracy. Digital compensation of sensitivity drift caused by package-induced stress is provided.

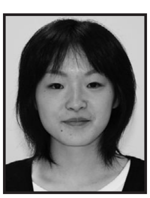

16.7 A 200dB Dynamic Range Iris-less CMOS Image Sensor with Lateral Overflow Integration Capacitor using Hybrid Voltage and Current Readout Operation **4:15 PM**

N. Akahane, Tohoku University, Sendai, Japan

A $2.6\times2.6mm^2$ image sensor fabricated in 0.35µm 2P3M CMOS contains 64×64 pixels with $20\times20\mu m^2$ pixel size and has an extended dynamic range of over 200dB. This DR is equivalent to the incident light ranging from about 10^{-2} to 10^8 lx with the lens iris fixed.

16.8 A Back-Illuminated High-Sensitivity Small-Pixel Color CMOS Image Sensor with Flexible Layout of Metal Wiring **4:45 PM**

S. Iwabuchi, Sony, Atsugi-shi, Japan

A 1.3Mpixel color image sensor with a back-illuminated configuration and 3.45µm square pixels is fabricated in 0.25µm 1P3M CMOS. Its sensitivity at a wavelength of 550nm is 34% better than that of a conventional device, and it falls by only 15% when the light is incident at an angle of 20 degrees. Flexibility in metal wiring layout improves device characteristics such as saturation output.

16.9 Laser Radar Imager Based on 3D Integration of Geiger-Mode Avalanche Photodiodes with Two SOI Timing Circuit Layers **5:00 PM**

B. Aull, MIT Lincoln Laboratory, Lexington, MA

A 64x64 laser-radar (ladar) detector array with 50µm pixel size measures the arrival times of single photons using Geiger-mode avalanche photodiodes (APD). A 3-tier structure with active devices on each tier is used with 227 transistors, six 3D vias and an APD in each pixel. A 9b pseudorandom counter in the pixel measures time. Initial imagery shows 2ns time quantization.